Aircraft Conflict Prediction in the Presence of a Spatially Correlated Wind Field

Jianghai Hu, *Member, IEEE*, Maria Prandini, *Member, IEEE*, and Shankar Sastry, *Fellow, IEEE*

***Abstract*—In this paper, the problem of automated aircraft conflict prediction is studied for two-aircraft midair encounters. A model is introduced to predict the aircraft positions along some look-ahead time horizon, during which each aircraft is trying to follow a prescribed flight plan despite the presence of additive wind perturbations to its velocity. A spatial correlation structure is assumed for the wind perturbations such that the closer the two aircraft, the stronger the correlation between the perturbations to their velocities. Using this model, a method is introduced to evaluate the criticality of the encounter situation by estimating the probability of conflict, namely, the probability that the two aircraft come closer than a minimum allowed distance at some time instant during the look-ahead time horizon. The proposed method is based on the introduction of a Markov chain approximation of the stochastic processes modeling the aircraft motions. Several generalizations of the proposed approach are also discussed.**

***Index Terms*—Air traffic control, conflict prediction, stochastic approximation, stochastic fields, stochastic modeling, wind correlation.**

I. Introduction

In the current air traffic management (ATM) system, air traffic controllers are in charge of guaranteeing safety by issuing to pilots correcting actions whenever a safety critical situation is predicted. The achievable capacity of the air traffic system is limited by the human-operated nature of this procedure, and it can be increased by introducing automatic tools to support air traffic controllers in detecting and resolving safety critical situations.

In this paper, among the many different safety critical situations that may occur in the ATM system, the authors focus on those midair "conflict" situations that arise when two aircraft flying at the same altitude come closer to each other than a minimum allowed distance, currently 5 nautical miles (nmi) in en route airspace and 3 nmi in airspace close to the airports [1].

Typically, the procedure used to prevent the occurrence of a conflict consists of two phases, namely, conflict detection and conflict resolution. See [2] for a comprehensive review on the automated tools proposed in the literature to support the air traffic controllers in performing these tasks. Roughly speaking, in the conflict detection phase, models for predicting the aircraft future positions are introduced, and the possibility that a conflict would occur within a certain time horizon is evaluated based on these models [3]–[6]. In the case that a conflict is predicted, the aircraft flight plans are modified in the conflict resolution phase so as to avoid the actual occurrence of the predicted conflict. When selecting the new flight plans, the cost of the resolution action in terms of, e.g., delay, fuel consumption, deviation from the originally planned itineraries, is usually taken into consideration [7]–[14].

In this paper, the conflict detection issue is studied and addressed from a probabilistic viewpoint. Two aircraft flying in some region of the airspace, each of which is following a certain flight plan, are considered. The aircraft actual motions differ from the planned ones due to various sources of uncertainty, primarily the wind. The objective here is to evaluate if the aircraft flight plans are safe by estimating the probability that a conflict will occur over some look-ahead time horizon. In practice, once a prescribed threshold value of the probability of conflict is surpassed, an alarm of corresponding severity should be issued to the air traffic controllers/pilots to warn them on the level of criticality of the situation [15].

There are several factors that, combined, make the problem of estimating the probability of conflict highly complicated and, as such, impossible to solve analytically. For example, in principle, the aircraft flight plans can be arbitrary motions; in fact, they are generally more complex than the simple planar linear motions assumed, e.g., in [5] and [16] when deriving analytic expressions of the probability of a two-aircraft conflict. In addition, and probably most importantly, the random wind perturbations to the aircraft motions are spatially correlated. This spatial correlation property of the wind field has been observed and studied at both the microscopic scale [17] and the mesoscopic scale [18]. Neglecting the wind spatial correlation can cause erroneous evaluations when computing the probability of conflict, since the closer two aircraft are to each other, the more correlated the wind perturbations to their motions; hence, it is more likely that these perturbations will cancel each other. However, although known to be a critical issue in aircraft conflict prediction [19], the wind spatial correlation is largely ignored in the current literature, probably due to the difficulty in its modeling and analysis. Indeed, the methods proposed in the literature to compute the probability of conflict are generally based on the two-aircraft model introduced in [4], where each aircraft motion is described as a Gaussian random process whose variance grows in time, and the processes modeling the motions of the two aircraft are assumed to be uncorrelated.

Manuscript received February 22, 2004; revised July 28, 2004. This work was partly supported by the European Commission under project HYBRIDGE IST-2001-32460 and by the National Science Foundation under Grant EIA-0122599. The Associate Editor for this paper was F.-Y. Wang.

J. Hu is with the Purdue University, West Lafayette, IN 47906, USA (e-mail: jianghai@purdue.edu).

M. Prandini is with the Politecnico di Milano, Milan, 20133, Italy (e-mail: prandini@elet.polimi.it).

S. Sastry is with the University of California, Berkeley, CA 94720, USA (e-mail: sastry@eecs.berkeley.edu).

Digital Object Identifier 10.1109/TITS.2005.853699

Inspired by [20], a model for a two-aircraft encounter consisting of a pair of coupled stochastic differential equations is introduced, where the correlation between the wind perturbations affecting the aircraft positions is taken into account. Specifically, in this model, the flight plan of each aircraft can be arbitrary; the aircraft actual motion may deviate from the planned one due to the presence of spatially correlated wind perturbations affecting the aircraft velocity additively. To a certain extent, this model is a simplified version of the one proposed in [20], which is interesting but too complicated for the purpose of computing the probability of conflict.

Based on this model, the probability of conflict is computed by introducing a Markov chain whose state space is obtained by discretizing the region of the airspace where the encounter occurs. With properly chosen transition probabilities, the Markov chain converges weakly to the stochastic processes modeling the aircraft motions as the grid size approaches zero. The probability of conflict can then be approximated by the corresponding quantity associated with the Markov chain. Numerical algorithms are presented for computing the probability of conflict map, which assigns to a pair of locations the probability that a conflict occurs within a certain look-ahead time horizon starting from a given time instant with the two aircraft being at those locations at that time instant. Simulation results confirm that the wind correlation effect cannot be ignored when estimating the probability of conflict.

The approximating Markov chain has a state space of dimension four, as each aircraft position at a fixed altitude can be identified by two coordinates in $\mathbb{R}^2$. Under some additional assumptions, the problem can be simplified and solved by referring to the relative position of the two aircraft and using an approximating Markov chain with a two-dimensional (2-D) state space, which greatly reduces the computation load.

The proposed approach can be extended to address encounters where the aircraft do not necessarily fly at the same fixed altitude and may perform vertical maneuvers. Work in this direction has been done in [21] for a simplified case where it suffices to track the relative position of the two aircraft to estimate their probability of conflict in three-dimensional (3-D) airspace.

Finally, it is remarked that the distinguishing feature of the proposed method for conflict prediction is its consideration of correlated wind effect when predicting the aircraft future positions. Thus, the performance of the approach cannot be directly compared with that of other probabilistic methods for conflict prediction in the literature [2], where wind correlation is neglected.

The rest of the paper is organized as follows. In Section II, the model of a two-aircraft encounter is described and the problem of computing the probability of conflict is formalized. A Markov chain approximation scheme is then proposed to estimate the probability of conflict, starting from a simplified case in Section III and then extending the approach to the general case in Section IV. Simulation results for both cases are also presented, which show that the probability of conflict depends on the wind spatial correlation structure. The extension of the proposed method to estimating the probability of intrusion for a single aircraft into a forbidden area of the airspace is briefly discussed in Section V. Finally, Section VI draws some conclusions and outlines future directions of research.

II. Model of the Aircraft Motion

In this section, a kinematic model of the aircraft motion to predict the aircraft future positions during the time interval $T = [0, t_f]$ is introduced, where 0 is the current time instant and $t_f \in (0, \infty)$ represents the look-ahead time horizon.

Consider an aircraft flying at a constant altitude. The airspace can then be identified with $\mathbb{R}^2$, and the aircraft position at time $t \in T$ can be denoted by a vector $X(t)$ in $\mathbb{R}^2$. The dynamics of $X(t)$ during the time interval T depends on the aircraft velocity profile and an additive perturbation term to the aircraft velocity. These two terms are detailed next.

It is assumed that during the time interval T, the aircraft is trying to follow a velocity profile $u: \mathbb{R}^2 \times T \to \mathbb{R}^2$, meaning that at time $t \in T$, the aircraft plans to fly at velocity $u(x,t)$ if its location at time t is $x \in \mathbb{R}^2$. The velocity profile u is the sum of two terms: a nominal velocity profile $u_n: T \to \mathbb{R}^2$ and a correction term $u_c: \mathbb{R}^2 \times T \to \mathbb{R}^2$, i.e., $u(x,t) = u_n(t) + u_c(x,t)$, $x \in \mathbb{R}^2$, $t \in T$. The nominal velocity profile u_n represents the aircraft flight plan, which is typically chosen to be a piecewise constant function, since it is a common practice in the ATM systems that aircraft are advised to travel at constant speed piecewise linear motions specified by a series of way-points. The correction term u_c models the feedback control action of the flight management system (FMS) trying to bring the aircraft back to its nominal path should a deviation occur due to some perturbations.

In addition to the velocity profile that is designated by the air traffic controller and by the onboard FMS, there are also various environmental factors that can affect the aircraft velocity. Among them, wind is a major one and is the one considered in this paper. Specifically, the wind contribution to the aircraft velocity is modeled as the sum of two terms: 1) a deterministic term $f: \mathbb{R}^2 \times T \to \mathbb{R}^2$ (called the wind field) representing the nominal wind velocity, which may depend on the aircraft location x and the time t, and is assumed to be known to the air traffic controller through measurements or forecast; and 2) a stochastic term representing the effect of air turbulence and errors in the wind speed measurements and forecast. The time integral of the stochastic term is modeled by a random field $B(\cdot,\cdot)$ on $\mathbb{R}^2 \times T$ with the following properties.

1) For each fixed $x \in \mathbb{R}^2$, $B(x,\cdot)$ is a standard 2-D Brownian motion.
2) $B(\cdot,\cdot)$ is time increment independent. This implies, in particular, that the collections of random variables $\{B(x,t_2)-B(x,t_1)\}_{x\in\mathbb{R}^2}$ and $\{B(x,t_4)-B(x,t_3)\}_{x\in\mathbb{R}^2}$ are independent for any $t_1, t_2, t_3, t_4 \in T$, with $t_1 \le t_2 \le t_3 \le t_4$.
3) $\{B(x,t_2) - B(x,t_1)\}_{x\in\mathbb{R}^2}$, for $t_1, t_2 \in T$ with $t_1 \le t_2$, is an (uncountable) collection of Gaussian random variables with zero mean and covariance

$$E\left\{[B(x,t_2) - B(x,t_1)]\,[B(y,t_2) - B(y,t_1)]^{\mathrm{T}}\right\} = h(x-y)(t_2-t_1)I_2 \quad \forall x, y \in \mathbb{R}^2$$

where I_2 is the 2×2 identity matrix and $h: \mathbb{R}^2 \to \mathbb{R}$ is a continuous function such that $h(0) = 1$, $h(x) = h(-x)\ \forall x \in \mathbb{R}^2$, and $h(x) \to 0$ as $x \to \infty$. In addition, h has to be nonnegative definite in the sense that the k-by-k matrix $[h(x_i - x_j)]_{i,j=1}^k$ is nonnegative definite for arbitrary $x_1, \ldots, x_k \in \mathbb{R}^2$ and positive integer k. In this paper, the spatial correlation function is taken to be $h(x) = \exp(-\beta\|x\|)$ for some $\beta > 0$, a popular choice for the random field models in geostatistics [22]. This choice is actually shown to be suitable for ATM applications in [19], where the wind field prediction made by the rapid update cycle (RUC) [23] developed at the National Oceanic and Atmospheric Administration (NOAA) Forecast System Laboratory (FOL) is compared with the empirical data collected by the Meteorological Data Collection Reporting System (MDCRS) near Denver International Airport. The result of this comparison is that an exponentially decaying function of the horizontal separation fits in very well with the spatial correlation statistics of the wind field prediction errors. A proof that such an exponentially decaying h is nonnegative definite can be found, e.g., in [24].

Remark 1: Typically, the wind field f is assumed to satisfy some continuity property. This condition, together with the monotonicity assumption on the spatial correlation function h, is introduced to model the fact that the closer two points in space are, the more similar the wind velocities at those points are, and as the two points move farther away from each other, the wind velocities become nearly independent.

The random field $B(\cdot, \cdot)$ is Gaussian, stationary in space (its finite dimensional distributions are invariant to shifts of the origin of $\mathbb{R}^2$), and isotropic (its finite dimensional distributions are invariant with respect to changes of orthonormal coordinates). A constructive proof of the existence of $B(\cdot, \cdot)$ with the desired properties can be found in the Appendix.

For later developments, it is convenient to write $B(\cdot, \cdot)$ in the Karthunen–Loeve expansion as

$$B(x,t) = \sum_{n=0}^{\infty} \sqrt{\lambda_n}\phi_n(x)B_n(t) \tag{1}$$

where $\{B_n(t)\}_{n\geq 0}$ is a series of independent 2-D standard Brownian motions, and $\{(\lambda_n, \phi_n(x))\}_{n\geq 0}$ is a complete set of eigenvalue and eigenfunction pairs for the integral operator $\phi(x) \mapsto \int_{\mathbb{R}^2} h(s-x)\phi(s)\mathrm{d}s$, i.e.,

$$\begin{cases} \lambda_n\phi_n(x) = \int_{\mathbb{R}^2} h(s-x)\phi_n(s)\mathrm{d}s \\ h(x-y) = \sum_{n=0}^{\infty} \lambda_n\phi_n(x)\phi_n(y) \end{cases} \quad \forall x, y \in \mathbb{R}^2. \tag{2}$$

Thus, the position X of the aircraft during the time horizon T is governed by the following stochastic differential equation

$$\mathrm{d}X(t) = u(X,t)\mathrm{d}t + f(X,t)\mathrm{d}t + g(X,t)\sum_{n=0}^{\infty} \sqrt{\lambda_n}\phi_n(X)\mathrm{d}B_n(t) \tag{3}$$

initialized with the aircraft current position $X(0)$. Recall that the aircraft velocity profile u is given by $u(x,t) = u_n(t) + u_c(x,t)$, and $f(x,t)$ is the wind field, $x \in \mathbb{R}^2$, $t \in T$. In addition, $g: \mathbb{R}^2 \times T \to \mathbb{R}^{2\times 2}$ is a matrix-valued function introduced to modulate the variances of the random wind perturbations along different directions.

In this paper, it is assumed for simplicity that $g \equiv \sigma I_2$ for some constant $\sigma > 0$. This implies in particular that the random contribution of the wind to the aircraft velocity after the modulation of g remains isotropic, which is a reasonable assumption considering that, in the proposed model, there is no apparent direction in $\mathbb{R}^2$ preferential to others.

Equation (3) is rewritten as

$$\mathrm{d}X(t) = u(X,t)\mathrm{d}t + f(X,t)\mathrm{d}t + \sigma\sum_{n=0}^{\infty} \sqrt{\lambda_n}\phi_n(X)\mathrm{d}B_n(t) \tag{4}$$

with the initial condition $X(0)$. The two-aircraft conflict prediction problem based on (4) is now described.

A. Two-Aircraft Conflict Prediction Problem

Consider two aircraft, say "aircraft 1" and "aircraft 2," flying at the same altitude during the time interval T. Denote their positions and their velocity profiles by X_i and u_i, $i = 1, 2$, respectively. Based on (4), the evolutions of $X_1(\cdot)$ and $X_2(\cdot)$ during T are governed by

$$\mathrm{d}X_1(t) = u_1(X_1,t)\mathrm{d}t + f(X_1,t)\mathrm{d}t + \sigma\sum_{n=0}^{\infty} \sqrt{\lambda_n}\phi_n(X_1)\mathrm{d}B_n(t) \tag{5}$$

$$\mathrm{d}X_2(t) = u_2(X_2,t)\mathrm{d}t + f(X_2,t)\mathrm{d}t + \sigma\sum_{n=0}^{\infty} \sqrt{\lambda_n}\phi_n(X_2)\mathrm{d}B_n(t) \tag{6}$$

starting from the initial positions $X_1(0)$ and $X_2(0)$.

A conflict occurs whenever the two aircraft get closer than r horizontally at some time $t \in T$. The objective here is to compute the probability of this event, namely

$$P_c \triangleq P\left\{\|X_2(t) - X_1(t)\| \leq r \text{ for some } t \in T\right\}.$$

P_c is referred to as the probability of conflict. Given that it is, in general, impossible to derive P_c analytically, the goal in this paper is then to design numerical algorithms to compute P_c.

III. Simplified Case

First, a simplified case where the computation of P_c can be especially efficient is considered.

Assumption 1: Assume that

1) the wind field $f(x,t)$ is affine in x, i.e.,

$$f(x,t) = R(t)x + \mathrm{d}(t) \quad \forall x \in \mathbb{R}^2, t \in T$$

where $R: T \to \mathbb{R}^{2\times 2}$ and $d: T \to \mathbb{R}^2$ are continuous;

2) the velocity profiles $u_1(x,t)$ and $u_2(x,t)$ depend only on t, not on x.

Under Assumption 1, (5) and (6) become

$$\begin{aligned}\mathrm{d}X_1(t) &= u_1(t)\mathrm{d}t + [R(t)X_1 + \mathrm{d}(t)]\,\mathrm{d}t \\ &\quad + \sigma\sum_{n=0}^{\infty}\sqrt{\lambda_n}\phi_n(X_1)\mathrm{d}B_n(t) \qquad (7)\\ \mathrm{d}X_2(t) &= u_2(t)\mathrm{d}t + [R(t)X_2 + \mathrm{d}(t)]\,\mathrm{d}t \\ &\quad + \sigma\sum_{n=0}^{\infty}\sqrt{\lambda_n}\phi_n(X_2)\mathrm{d}B_n(t). \qquad (8)\end{aligned}$$

It is shown next that it suffices to study the problem in the relative coordinate system, which effectively reduces the state space dimension of the problem to two.

Denote by Y and v the relative position and the relative velocity profile of the two aircraft

$$Y(t) \triangleq X_2(t) - X_1(t), \quad v(t) \triangleq u_2(t) - u_1(t).$$

Then, the probability of conflict can be expressed as

$$P_c = P\left\{\|Y(t)\| \le r \text{ for some } t \in T\right\}.$$

Moreover, subtracting (7) from (8) yields

$$\begin{aligned}\mathrm{d}Y(t) &= v(t)\mathrm{d}t + R(t)Y(t)\mathrm{d}t \\ &\quad + \sigma\sum_{n=0}^{\infty}\sqrt{\lambda_n}\left[\phi_n(X_2) - \phi_n(X_1)\right]\mathrm{d}B_n(t). \qquad (9)\end{aligned}$$

Fix $x_1, x_2 \in \mathbb{R}^2$ and let $y = x_2 - x_1$. Define

$$Z(t) \triangleq \sum_{n=0}^{\infty}\sqrt{\lambda_n}\left[\phi_n(x_2) - \phi_n(x_1)\right]B_n(t). \qquad (10)$$

$Z(t)$ is a Gaussian process with zero mean and covariance

$$E\left\{[Z(t_2)-Z(t_1)]\,[Z(t_2)-Z(t_1)]^{\mathrm{T}}\right\} = 2\,[1-h(y)]\,(t_2-t_1)I_2$$

for $t_1 \le t_2$, where the last equation follows from (2) and the fact that $h(0) = 1$. Note also that $Z(0) = 0$. Therefore, in terms of distribution

$$Z(t) \stackrel{d}{=} \sqrt{2\,[1-h(y)]}\,W(t) \qquad (11)$$

where $W(t)$ is a standard 2-D Brownian motion.

Consider now the stochastic differential equation

$$\mathrm{d}\bar{Y}(t) = v(t)\mathrm{d}t + R(t)\bar{Y}(t)\mathrm{d}t + \sigma\sqrt{2\left[1-h(\bar{Y})\right]}\,\mathrm{d}W(t) \qquad (12)$$

initialized with $\bar{Y}(0) = Y(0)$. In view of (10) and (11), $Y(t)$ has the same distribution as $\bar{Y}(t)$. Then, the probability of conflict P_c can be determined as

$$P_c = P\left\{\bar{Y}(t) \in D \text{ for some } t \in T\right\}$$

where $D \subset \mathbb{R}^2$ is the closed disk of radius r centered at the origin modeling the protection zone surrounding each aircraft.

In order to compute the probability of conflict numerically, choose an open domain $U \subset \mathbb{R}^2$ with compact support containing D. U should be large enough so that the situation can be declared safe once the relative position of the two aircraft wanders outside U. With reference to the domain U, the probability of conflict can be approximated by

$$P_c^U \triangleq P\{\bar{Y} \text{ hits } D \text{ before hitting } U^c \text{ within } T\}. \qquad (13)$$

Implicit in the above definition is that if $\bar{Y}$ hits neither D nor U^c during T, still no conflict occurs. To compute P_c^U, (12) can now be considered, where $\bar{Y}$ is defined on the open domain $U \setminus D$ with initial condition $Y(0)$ and is stopped as soon as it hits the boundary $\partial U \cup \partial D$.

A. Markov Chain Approximation

An approach to approximate the solution $\bar{Y}(\cdot)$ to (12) defined on $U \setminus D$ is now described. The idea is to discretize $U \setminus D$ into grids that constitute the state space of a Markov chain. By carefully choosing the transition probabilities, the solution to the Markov chain will converge weakly to that of (12) as the grid size approaches zero. Therefore, at a small grid size, a good estimate of P_c^U is provided by the corresponding quantity associated with the Markov chain, which can be computed numerically.

Some notations are needed to define the Markov chain. Fix a grid size $\delta > 0$. Denote by $\delta\mathbb{Z}^2$ the integer grids of $\mathbb{R}^2$ scaled by δ, namely, $\delta\mathbb{Z}^2 = \{(m\delta, n\delta) | m, n \in \mathbb{Z}\}$. Each grid point in $\delta\mathbb{Z}^2$ has four immediate neighbors (left, right, down, and up positions). Define $S = (U \setminus D) \cap \delta\mathbb{Z}^2$, which consists of all those grid points in $\delta\mathbb{Z}^2$ that lie inside U but outside D. The interior of S, denoted by S^0, consists of all those points in S whose all four neighbors in $\delta\mathbb{Z}^2$ belong to S as well. The boundary of S is defined to be $\partial S = S \setminus S^0$, and is the union of two disjoint sets: $\partial S = \partial S_U \cup \partial S_D$, where points in ∂S_U have at least one neighbor outside U, and points in ∂S_D have at least one neighbor inside D.

A time-inhomogeneous Markov chain $\{Q_k, k \ge 0\}$ can now be defined on the state space S as follows.

1) States in ∂S are absorbing, i.e., the chain remains unchanged upon arriving at any of the states in ∂S.
2) Starting from a state q in S^0, the chain jumps to one of its four neighbors: $q_l = q + (-\delta, 0)$, $q_r = q + (\delta, 0)$, $q_d = q + (0, -\delta)$, and $q_u = q + (0, \delta)$, or stays at q according to transition probabilities determined by its current location q and the current time step k as

$$P\{Q_{k+1} = q' \,|\, Q_k = q\} = \begin{cases} p_l^k(q) = \frac{\exp\left(-\delta\xi_q^k\right)}{C_q^k}, & q' = q_l \\ p_r^k(q) = \frac{\exp\left(\delta\xi_q^k\right)}{C_q^k}, & q' = q_r \\ p_d^k(q) = \frac{\exp\left(-\delta\eta_q^k\right)}{C_q^k}, & q' = q_d \\ p_u^k(q) = \frac{\exp\left(\delta\eta_q^k\right)}{C_q^k}, & q' = q_u \\ p_o^k(q) = \frac{\chi_q^k}{C_q^k}, & q' = q \\ 0, & \text{otherwise.} \end{cases} \qquad (14)$$

The parameters in the above expression are given by

$$\xi_q^k = \frac{[v(k\Delta t) + R(k\Delta t)q]_1}{2\sigma^2\,[1-h(q)]}$$
$$\eta_q^k = \frac{[v(k\Delta t) + R(k\Delta t)q]_2}{2\sigma^2\,[1-h(q)]}$$
$$\chi_q^k = \frac{1}{\lambda\sigma^2\,[1-h(q)]} - 4$$
$$C_q^k = 2\mathrm{csh}\left(-\delta\xi_q^k\right) + 2\mathrm{csh}\left(-\delta\eta_q^k\right) + \chi_q^k$$

where for an arbitrary vector $z \in \mathbb{R}^2$, $[z]_i$ denotes its ith component with $i = 1, 2$. λ is a positive constant small enough such that χ_q^k defined above is positive for all q and all k. In particular, this is guaranteed if $0 < \lambda \leq (4\sigma^2)^{-1}$. $\Delta t > 0$ is the amount of time elapsed between any two successive discrete time steps k and $k+1$, $k \geq 0$. Here, $\Delta t = \lambda\delta^2$.

Suppose that at time step k, the chain is at $q \in S^0$. Define

$$m_q^k = \frac{1}{\Delta t} E\{Q_{k+1} - Q_k | Q_k = q\}$$
$$V_q^k = \frac{1}{\Delta t} E\left\{(Q_{k+1} - Q_k)(Q_{k+1} - Q_k)^{\mathrm{T}} | Q_k = q\right\}.$$

Direct computation shows that

$$m_q^k = \frac{2}{\lambda\delta C_q^k}\begin{bmatrix}\mathrm{sh}\left(\delta\xi_q^k\right)\\ \mathrm{sh}\left(\delta\eta_q^k\right)\end{bmatrix}$$
$$V_q^k = \frac{2}{\lambda C_q^k}\begin{bmatrix}\mathrm{csh}\left(\delta\xi_q^k\right) & 0\\ 0 & \mathrm{csh}\left(\delta\eta_q^k\right)\end{bmatrix}.$$

If for each $\delta > 0$, q is chosen to be a point in S^0 closest to a fixed point $y \in U \setminus D$, then one can verify that, as $\delta \to 0$

$$m_q^k \to v(k\Delta t) + R(k\Delta t)y$$
$$V_q^k \to 2\sigma^2\,[1-h(y)]\,I_2.$$

Assume that the chain starts from a point $\bar{q} \in S$ closest to $Y(0)$. Then, by Theorem 8.7.1 in [25] (see also [26]), the following holds.

Proposition 1: Fix $\delta > 0$ and consider the corresponding Markov chain $\{Q_k, k \geq 0\}$. Denote by $\{Q(t), t \geq 0\}$ the stochastic process that is equal to Q_k on the time interval $[k\Delta t, (k+1)\Delta t)$ for all k. Then, as $\delta \to 0$, $\{Q(t), t \geq 0\}$ converges weakly to the solution $\{\bar{Y}(t), t \geq 0\}$ to (12) defined on $U \setminus D$ with absorption on the boundary $\partial U \cup \partial D$.

Let $k_f \triangleq \lfloor t_f/\Delta t \rfloor$ be the largest integer not exceeding $t_f/\Delta t$. Due to the weak convergence of $Q(t)$ to $\bar{Y}(t)$, for small δ, the probability P_c^U in (13) can be approximated by the corresponding probability

$$P_{c,\delta}^U \triangleq P\left\{Q_{k_f} \in \partial S_D\right\} = P\{Q_k \text{ hits } \partial S_D \text{ before hitting } \partial S_U \text{ within } 0 \leq k \leq k_f\} \quad (15)$$

with Q_k starting from a point $\bar{q} \in S$ closest to $Y(0)$.

Remark 2: In a single time step of duration $\Delta t = \lambda\delta^2$, the maximal distance that the Markov chain can travel is a unitary grid step δ. Thus, given $v(t)$, $R(t)$, and U, in order for $\bar{Y}(t)$ to be approximated by the Markov chain, the quantity $\|v(t) + R(t)y\|$, $t \in T$, $y \in U$, has to be upper bounded roughly by $1/\lambda\delta$, which is $4\sigma^2/\delta$ if λ is chosen to be $(4\sigma^2)^{-1}$. This condition translates into an upper bound on the admissible values of δ. In other words, fast diffusion process $\bar{Y}(t)$ cannot be simulated by Markov chains corresponding to large δ's.

Remark 3: The Markov chain approximation described above still applies with suitable modifications to the case when the velocity profiles of the two aircraft depend affinely on x with identical matrices multiplying the x variable.

B. Numerical Algorithm

The algorithm to compute $P_{c,\delta}^U$ is described next. For each $q \in S$ and $k = 0, 1, \ldots, k_f$, define

$$P_{c,\delta}^{(k)}(q) \triangleq P\left\{Q_{k_f} \in \partial S_D | Q_k = q\right\}. \quad (16)$$

The set of functions $P_{c,\delta}^{(k)}: S \to \mathbb{R}$, $0 \leq k \leq k_f$, satisfies the following recursive (Kolmogorov backward) equation

$$P_{c,\delta}^{(k)}(q) = \begin{cases} P_{c,\delta,\mathrm{new}}^{(k)}(q), & \text{if } q \in S^0\\ 1, & \text{if } q \in \partial S_D\\ 0, & \text{if } q \in \partial S_U\end{cases} \quad (17)$$

with boundary condition

$$P_{c,\delta}^{(k_f)}(q) = \begin{cases} 1, & \text{if } q \in \partial S_D\\ 0, & \text{otherwise}\end{cases} \quad (18)$$

where in (17), $P_{c,\delta,\mathrm{new}}^{(k)}(q)$ is defined by

$$P_{c,\delta,\mathrm{new}}^{(k)}(q) = p_o^k(q)P_{c,\delta}^{(k+1)}(q) + p_l^k(q)P_{c,\delta}^{(k+1)}(q_l) + p_r^k(q)P_{c,\delta}^{(k+1)}(q_r) + p_d^k(q)P_{c,\delta}^{(k+1)}(q_d) + p_u^k(q)P_{c,\delta}^{(k+1)}(q_u).$$

In particular, $P_{c,\delta}^{(0)}$ can be computed recursively by iterating k_f times the backward equation (17) initialized with (18). The desired quantity $P_{c,\delta}^U$ defined in (15) is then $P_{c,\delta}^{(0)}(\bar{q})$. The following algorithm summarizes the overall procedure.

Algorithm 1. For given $Y(0)$, $v(t)$, and $R(t)$, $t \in T$:

1) Fix $\delta > 0$ and $\lambda \in (0, 1/(4\sigma^2)]$. Set $\Delta t = \lambda\delta^2$. Define $\{Q_k, k \geq 0\}$ to be the Markov chain with state space $S = (U \setminus D) \cap \delta\mathbb{Z}^2$ and transition probabilities (14).
2) Initialize $P_{c,\delta}^{(k_f)}$ according to (18).
3) For $k = k_f - 1, \ldots, 0$, compute $P_{c,\delta}^{(k)}$ from $P_{c,\delta}^{(k+1)}$ according to (17).
4) Output $P_{c,\delta}^U = P_{c,\delta}^{(0)}(\bar{q})$ for $\bar{q} \in S$ closest to $Y(0)$.

Remark 4: For a grid size δ, the size of the state space S is of the order of $1/\delta^2$. Since the number of iterations is given by $k_f \simeq t_f/\Delta t = O(1/\delta^2)$ and each iteration takes $O(1/\delta^2)$ time, the running time of Algorithm 1 grows as $O(1/\delta^4)$ as $\delta \to 0$. Therefore, small δ's may result in exceedingly long running

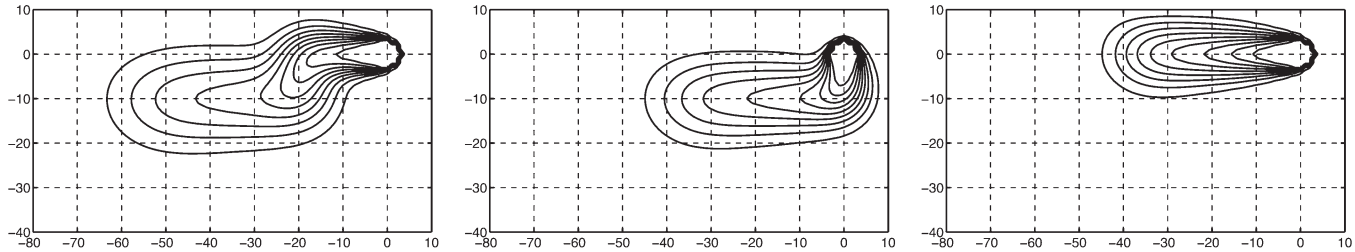

Fig. 1. Level curves of the estimated probability of conflict over the time horizon $T = [t, 40]$ as a function of the aircraft relative position at time $t = 0$, 10, 20 ($\beta = 1/5$).

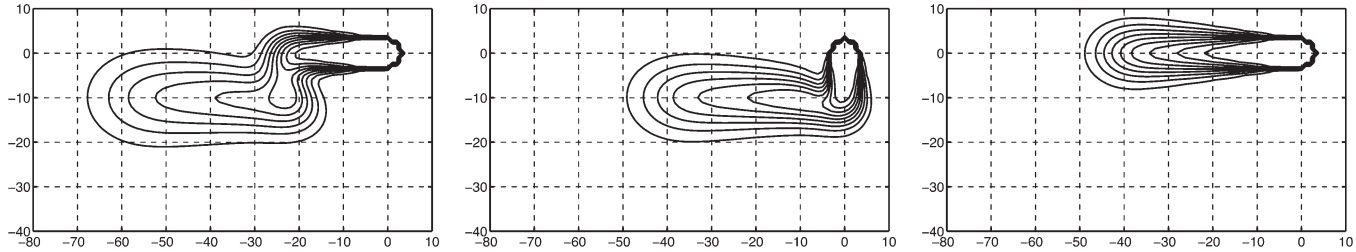

Fig. 2. Level curves of the estimated probability of conflict over the time horizon $[t, 40]$ as a function of the aircraft relative position at time $t = 0$, 10, 20 ($\beta = 1/20$).

time. On the other hand, as pointed out in Remark 2, large δ's may not allow for the simulation of fast moving processes and may lead to rough estimates. A suitable δ is then a compromise between these conflicting requirements.

Remark 5: Algorithm 1 determines the whole family of functions $P_{c,\delta}^{(k)}: S \to \mathbb{R}$, $k = 0, 1, \ldots, k_f$, in a single run. Hence, at any future time $t \in [0, t_f]$, should the aircraft velocity profiles be unchanged, an estimate of the probability of conflict over the new time horizon $[t, t_f]$ is readily available, eliminating the need for a recomputation.

C. Extension to the Case When the Aircraft Current Positions are Uncertain

The procedure for estimating P_c^U described above can be extended to the case where the aircraft current positions $X_1(0)$ and $X_2(0)$ are not known precisely. If $X_1(0)$ and $X_2(0)$ are described as random variables with a certain joint distribution, then the initial relative position $Y(0)$ is also a random variable with a certain distribution μ_Y on $U \setminus D$. Define

$$p_c^U(y) \triangleq P\{Y \text{ hits } D \text{ before hitting } U^c \text{ in } T | Y(0) = y\}$$

for $y \in U \setminus D$, which is the probability of conflict over the time horizon T when the initial relative position $Y(0)$ of the two aircraft is equal to $y \in U \setminus D$. Then, the probability of conflict can be expressed in terms of p_c^U as $\int_{U \setminus D} p_c^U(y) \mathrm{d}\mu_Y(y)$. This integral reduces to a finite summation when the state space $U \setminus D$ is discretized and p_c^U is approximated by $P_{c,\delta}^{(0)}$.

D. Examples

Algorithm 1 is now illustrated by some examples. Unless otherwise stated, the following parameters are used in the examples. The safe distance is $r = 3$; σ and h in (12) are, respectively, $\sigma = 1$ and $h(x) = \exp(-\beta\|x\|)$ $\forall x \in \mathbb{R}^2$, with $\beta > 0$; $T = [0, 40]$. The relative velocity profile of the two aircraft during the time horizon T is given by

$$v(t) = \begin{cases} (2, 0), & 0 \le t < 10 \\ (0, 1), & 10 \le t < 20 \\ (2, 0), & 20 \le t \le 40. \end{cases}$$

Based on T and $v(t)$, the domain U is chosen to be the rectangle $(-80, 10) \times (-40, 10)$. Finally, $\lambda = (4\sigma^2)^{-1} = 0.25$ and $\delta = 1$. In all the plots of the estimated probability of conflict, the reported level curves correspond to values 0.1, 0.2, . . ., 0.9, moving from the largest curves to the smallest one.

Example 1: Suppose that the wind field is identically zero: $R(t) \equiv 0$, $d(t) \equiv 0$ $\forall t \in T$. Let $\beta = 1/5$ so that $h(x) = \exp(-\|x\|/5)$ for $x \in \mathbb{R}^2$. By executing Algorithm 1, the set of functions $P_{c,\delta}^{(k)}: S \to [0, 1]$, $k = 0, 1, \ldots, k_f$ is computed. In Fig. 1 the level curves of $P_{c,\delta}^{(\lfloor t/\Delta t \rfloor)}$ are plotted at $t = 0$, $t = 10$, and $t = 20$, respectively, from left to right. Recall that $P_{c,\delta}^{(\lfloor t/\Delta t \rfloor)}$ represents an estimate of the probability of conflict over the time horizon $[t, t_f]$ as a function of the aircraft relative position at time t. As one can expect, the probability of conflict over $[t, t_f]$ has peak values along a nominal path traced by a point starting from the origin at time $t_f = 40$ and moving backward in time according to the nominal relative velocity $v(\cdot)$ until time t. The probability of conflict decreases as the relative position between the aircraft at time t moves farther away from that path. Furthermore, experiments (not reported here) show that the smaller the variance parameter σ is, the faster this decrease is.

Example 2: This example differs from the previous one only in the value of β, which is now $\beta = 1/20$. So $h(x) = \exp(-\|x\|/20)$ $\forall x \in \mathbb{R}^2$, implying a stronger correlation between the random wind perturbations to the two aircraft velocities than in Example 1. In Fig. 2, the level curves of $P_{c,\delta}^{(\lfloor t/\Delta t \rfloor)}$

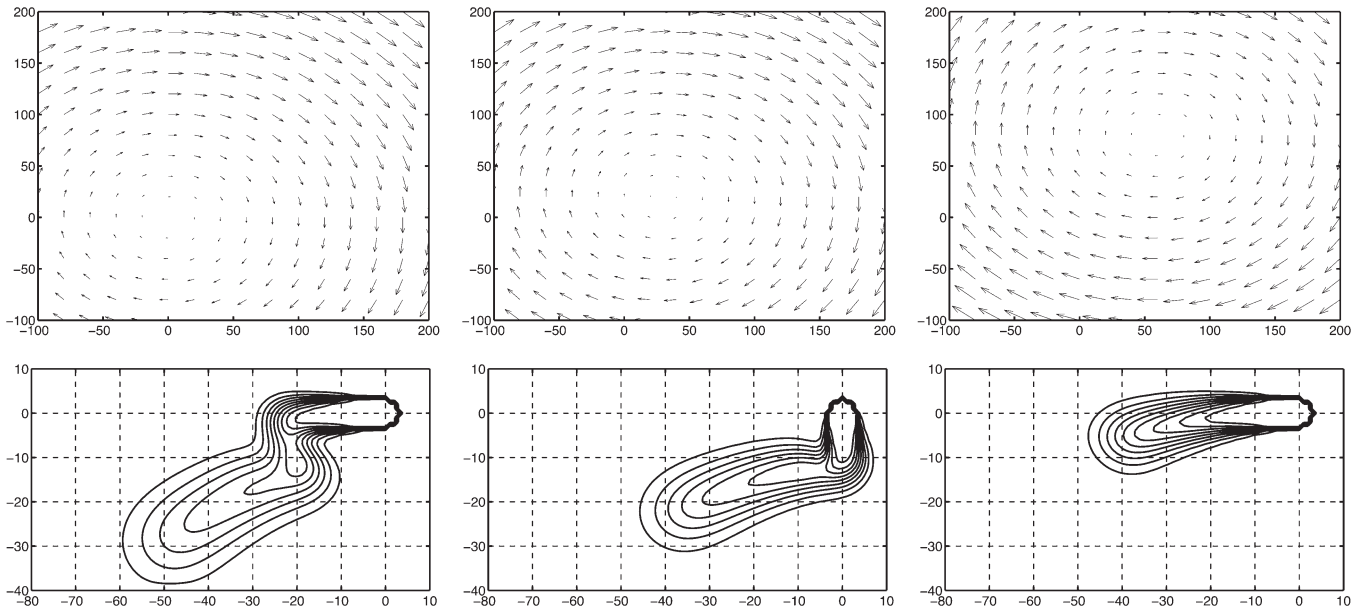

Fig. 3. Wind field (top) and level curves of the estimated probability of conflict over the time horizon $[t, 40]$ as a function of the aircraft relative position (bottom) at time $t = 0$, 10, 20 ($\beta = 1/20$).

computed by Algorithm 1 are plotted for $t = 0$, $t = 10$, and $t = 20$, from left to right. One can see that, compared to the plots in Fig. 1, the regions with higher probability of conflict in Fig. 2 are more concentrated along the nominal path, which is especially evident near the origin. The intuitive explanation of this phenomenon is that random wind perturbations to the aircraft velocities with larger correlation are more likely to cancel each other in the relative coordinates, resulting in more predictable behaviors and, hence, smaller probability of conflict outside the nominal collision course. In a sense, this implies that those approaches where the probability of conflict is estimated under the assumption of independent wind perturbations to the aircraft velocities could be pessimistic.

Example 3: In this example, $\beta = 1/20$ is chosen as in Example 2. However, it is assumed that there is a nontrivial affine wind field f defined by

$$f(x,t) = R(t)\left[x - z(t)\right], \quad x \in \mathbb{R}^2,\ t \in [0, 40]$$

where

$$R(t) = \frac{1}{50}\begin{bmatrix} 0 & 1 \\ -1 & 0 \end{bmatrix} \quad z(t) = \begin{bmatrix} 3t \\ \frac{t^2}{5} \end{bmatrix}.$$

The wind field f can be viewed as a windstorm swirling clockwise, whose center $z(t)$ accelerates along a parabolic curve during T. In fact, the choice of $z(t)$ has no effect on the probability of conflict since it will be canceled out in the relative coordinates. In the first row of Fig. 3, the wind field f on the region $[-100, 200] \times [-100, 200]$ is plotted at the time instants $t = 0$, 10, 20, from left to right. In the second row, the level curves of $P_{c,\delta}^{(\lfloor t/\Delta t \rfloor)}$ are plotted, where $t = 0$, 10, 20, from left to right. One can see that, compared to the results in Fig. 2, the regions with high probability of conflict are "bent" counterclockwise, and the farther away from the origin, the more the bending. This is because the net effect of the wind field f on the relative velocity v of the two aircraft when they are at the relative position y is Ry, which points clockwise when y is in the third quarter of the plane.

IV. General Case

In this section, the approach described in the previous section for estimating the probability of conflict is extended to the general case where Assumption 1 does not necessarily hold. Namely, the wind field $f(x,t)$ may not be affine in space, and/or the velocity profiles $u_1(x,t)$ and $u_2(x,t)$ may depend on x. The idea is still to use a Markov chain approximation method. However, in this general case, one has to keep track of each aircraft position, not simply their relative position, which causes the dimension of the state space of the introduced Markov chain to be four instead of two.

Consider the model of a two-aircraft encounter described in Section II, where the motions $X_1(\cdot)$ and $X_2(\cdot)$ of the aircraft are governed by (5) and (6), respectively.

Define

$$\hat{X} = \begin{bmatrix} X_1 \\ X_2 \end{bmatrix} \in \mathbb{R}^4.$$

Then, (5) and (6) can be written in terms of $\hat{X}$ as a single stochastic differential equation

$$\mathrm{d}\hat{X}(t) = \hat{u}(\hat{X},t)\mathrm{d}t + \hat{f}(\hat{X},t)\mathrm{d}t + \sigma\sum_{n=0}^{\infty}\sqrt{\lambda_n}\hat{\phi}_n(\hat{X})\mathrm{d}B_n(t) \tag{19}$$

where

$$\hat{u}(\hat{x},t)=\begin{bmatrix}u_1(x_1,t)\\ u_2(x_2,t)\end{bmatrix}$$
$$\hat{f}(\hat{x},t)=\begin{bmatrix}f(x_1,t)\\ f(x_2,t)\end{bmatrix}$$
$$\hat{\phi}_n(\hat{x})=\begin{bmatrix}\phi_n(x_1)I_2\\ \phi_n(x_2)I_2\end{bmatrix}$$

for $\hat{x}=\left[\begin{smallmatrix}x_1\\ x_2\end{smallmatrix}\right]\in\mathbb{R}^4$ and $t\in T$. The probability of conflict is

$$P_c\triangleq P\left\{\hat{X}(t)\in F \text{ for some } t\in T\right\}$$

where the set F is defined as

$$F\triangleq\left\{\hat{x}=\begin{bmatrix}x_1\\ x_2\end{bmatrix}\in\mathbb{R}^4:\ x_1,x_2\in\mathbb{R}^2,\|x_1-x_2\|\le r\right\}.$$

Fix $\hat{x}\in\mathbb{R}^4$ and define

$$Z(t)\triangleq\sum_{n=0}^{\infty}\sqrt{\lambda_n}\hat{\phi}_n(\hat{x})\mathrm{d}B_n(t). \tag{20}$$

$Z(t)$ is a Gaussian process with zero mean and covariance

$$E\left\{[Z(t_2)-Z(t_1)]\,[Z(t_2)-Z(t_1)]^{\mathrm{T}}\right\}=\begin{bmatrix}I_2 & \hat{h}(\hat{x})I_2\\ \hat{h}(\hat{x})I_2 & I_2\end{bmatrix}(t_2-t_1)\quad\forall t_1\le t_2$$

with $\hat{h}(\hat{x})\triangleq h(x_2-x_1)$, where $\hat{x}=(x_1,x_2)$. Note also that $Z(0)=0$. Therefore, in terms of distribution

$$Z(t)\overset{d}{=}\Sigma(\hat{x})\hat{W}(t)$$

where $\hat{W}(t)$ is a standard Brownian motion in $\mathbb{R}^4$ and

$$\Sigma(\hat{x})\triangleq\begin{bmatrix}I_2 & \hat{h}(\hat{x})I_2\\ \hat{h}(\hat{x})I_2 & I_2\end{bmatrix}^{\frac{1}{2}}\in\mathbb{R}^{4\times4}.$$

As a result, the process $\hat{X}$ solving (19) initialized with $\hat{X}(0)$ has the same distribution as the process $\bar{X}$ solving

$$\mathrm{d}\bar{X}(t)=\hat{u}(\bar{X},t)\mathrm{d}t+\hat{f}(\bar{X},t)\mathrm{d}t+\sigma\Sigma(\bar{X})\mathrm{d}\hat{W}(t) \tag{21}$$

with $\bar{X}(0)=\hat{X}(0)$, and the probability of conflict becomes

$$P_c=P\left\{\bar{X}(t)\in F \text{ for some } t\in T\right\}.$$

To evaluate numerically the probability of conflict, choose bounded open regions V_1 and V_2 of $\mathbb{R}^2$ large enough so that whenever the state $\bar{X}$ wanders outside $V\triangleq V_1\times V_2$, the situation can be declared to be safe. The quantity of interest then becomes

$$P_c^V\triangleq P\{\bar{X}\text{ hits }F\text{ before hitting }V^c\text{within the time interval }T\} \tag{22}$$

where $\bar{X}$ is the solution to (21) on the open set $V\setminus F$ with the initial condition $\hat{X}(0)=(X_1(0),X_2(0))\in V\setminus F$ and absorption on the boundary $\partial V\cup\partial F$.

A. Markov Chain Approximation

Proceed now as in Section III. For each $\delta>0$, let $\delta\mathbb{Z}^4$ be the integer grid in $\mathbb{R}^4$ scaled by δ, i.e., $\delta\mathbb{Z}^4=\{(i\delta,j\delta,m\delta,n\delta)|i,j,m,n\in\mathbb{Z}\}$. Each q in $\delta\mathbb{Z}^4$ has the following eight neighbors: $q_{ll}=q+(-\delta,0,-\delta,0)$, $q_{rr}=q+(\delta,0,\delta,0)$, $q_{lr}=q+(-\delta,0,\delta,0)$, $q_{rl}=q+(\delta,0,-\delta,0)$, $q_{dd}=q+(0,-\delta,0,-\delta)$, $q_{uu}=q+(0,\delta,0,\delta)$, $q_{du}=q+(0,-\delta,0,\delta)$, and $q_{ud}=q+(0,\delta,0,-\delta)$.

Define a Markov chain $\{Q_k,k\ge0\}$ with state space $S\triangleq(V\setminus F)\cap\delta\mathbb{Z}^4$. Denote by S^0 the interior of S consisting of those points in S whose eight neighbors in $\delta\mathbb{Z}^4$ all belong to S. Let ∂S_V be the set of points in S with at least one neighbor outside V, and let ∂S_F be the set of points in S with at least one neighbor inside F. If a point in S satisfies both these two conditions, then it is assigned only to ∂S_F. This will lead to an overestimation of P_c^V. However, if V_1 and V_2 are chosen to be large enough, this effect on the estimate of P_c^V can become negligible. The union $\partial S\triangleq\partial S_V\cup\partial S_F=S\setminus S^0$ of the two disjoint sets ∂S_V and ∂S_F is the boundary of S.

Suppose that each state in ∂S is an absorbing state for $\{Q_k,k\ge0\}$, and starting from an arbitrary state q in S^0 at time step $k\ge0$, the chain stays at the same state or jumps to one of its eight neighbors listed above according to the following transition probabilities

$$P\{Q_{k+1}=q'|Q_k=q\}=\begin{cases}p_{oo}^k(q)=\frac{\chi}{\chi+4}, & q'=q\\ p_{ll}^k(q)=\frac{\left(1+\alpha_q^k\right)\exp\left(-\delta\xi_q^k\right)}{\left[1+\exp\left(-\delta\xi_q^k\right)\right](\chi+4)}, & q'=q_{ll}\\ p_{rr}^k(q)=\frac{1+\alpha_q^k}{\left[1+\exp\left(-\delta\xi_q^k\right)\right](\chi+4)}, & q'=q_{rr}\\ p_{lr}^k(q)=\frac{1-\alpha_q^k}{\left[1+\exp\left(-\delta\eta_q^k\right)\right](\chi+4)}, & q'=q_{lr}\\ p_{rl}^k(q)=\frac{\left(1-\alpha_q^k\right)\exp\left(-\delta\eta_q^k\right)}{\left[1+\exp\left(-\delta\eta_q^k\right)\right](\chi+4)}, & q'=q_{rl}\\ p_{dd}^k(q)=\frac{\left(1+\alpha_q^k\right)\exp\left(-\delta\mu_q^k\right)}{\left[1+\exp\left(-\delta\mu_q^k\right)\right](\chi+4)}, & q'=q_{dd}\\ p_{uu}^k(q)=\frac{1+\alpha_q^k}{\left[1+\exp\left(-\delta\mu_q^k\right)\right](\chi+4)}, & q'=q_{uu}\\ p_{du}^k(q)=\frac{1-\alpha_q^k}{\left[1+\exp\left(-\delta\nu_q^k\right)\right](\chi+4)}, & q'=q_{du}\\ p_{ud}^k(q)=\frac{\left(1-\alpha_q^k\right)\exp\left(-\delta\nu_q^k\right)}{\left[1+\exp\left(-\delta\nu_q^k\right)\right](\chi+4)}, & q'=q_{ud}\\ 0, & \text{otherwise}\end{cases} \tag{23}$$

whose parameters are specified by

$$\begin{aligned}
\chi &= \frac{2}{\lambda\sigma^2} - 4 \\
\alpha_q^k &= \hat{h}(q) \\
\xi_q^k &= \frac{2}{\sigma^2\left(1+\alpha_q^k\right)}\left\{\left[\hat{f}(q,k\Delta t)+\hat{u}(q,k\Delta t)\right]_3 \right. \\
&\qquad \left. + \left[\hat{f}(q,k\Delta t)+\hat{u}(q,k\Delta t)\right]_1\right\} \\
\eta_q^k &= \frac{1}{\sigma^2\left(1-\alpha_q^k\right)}\left\{\left[\hat{f}(q,k\Delta t)+\hat{u}(q,k\Delta t)\right]_3 \right. \\
&\qquad \left. - \left[\hat{f}(q,k\Delta t)+\hat{u}(q,k\Delta t)\right]_1\right\} \\
\mu_q^k &= \frac{2}{\sigma^2\left(1+\alpha_q^k\right)}\left\{\left[\hat{f}(q,k\Delta t)+\hat{u}(q,k\Delta t)\right]_4 \right. \\
&\qquad \left. + \left[\hat{f}(q,k\Delta t)+\hat{u}(q,k\Delta t)\right]_2\right\} \\
\nu_q^k &= \frac{2}{\sigma^2\left(1-\alpha_q^k\right)}\left\{\left[\hat{f}(q,k\Delta t)+\hat{u}(q,k\Delta t)\right]_4 \right. \\
&\qquad \left. - \left[\hat{f}(q,k\Delta t)+\hat{u}(q,k\Delta t)\right]_2\right)\Big\}.
\end{aligned}$$

Here, $[z]_i$ denotes the ith component of a vector $z \in \mathbb{R}^4$, $1 \le i \le 4$. λ satisfies $0 < \lambda \le (2\sigma^2)^{-1}$. Δt is the time elapsed between successive discrete time steps and Δt is set equal to $\lambda\delta^2$.

For each $q \in S^0$ and each $k \ge 0$, define

$$\begin{aligned}
m_q^k &= \frac{1}{\Delta t}E\{Q_{k+1}-Q_k|Q_k=q\} \\
V_q^k &= \frac{1}{\Delta t}E\left\{(Q_{k+1}-Q_k)(Q_{k+1}-Q_k)^{\mathrm{T}}|Q_k=q\right\}.
\end{aligned}$$

Then, it can be verified that

$$m_q^k = \frac{\begin{bmatrix}
\left(1+\alpha_q^k\right)\frac{1-\exp\left(-\delta\xi_q^k\right)}{1+\exp\left(-\delta\xi_q^k\right)} - \left(1-\alpha_q^k\right)\frac{1-\exp\left(-\delta\eta_q^k\right)}{1+\exp\left(-\delta\eta_q^k\right)} \\
\left(1+\alpha_q^k\right)\frac{1-\exp\left(-\delta\mu_q^k\right)}{1+\exp\left(-\delta\mu_q^k\right)} - \left(1-\alpha_q^k\right)\frac{1-\exp\left(-\delta\nu_q^k\right)}{1+\exp\left(-\delta\nu_q^k\right)} \\
\left(1+\alpha_q^k\right)\frac{1-\exp\left(-\delta\xi_q^k\right)}{1+\exp\left(-\delta\xi_q^k\right)} + \left(1-\alpha_q^k\right)\frac{1-\exp\left(-\delta\eta_q^k\right)}{1+\exp\left(-\delta\eta_q^k\right)} \\
\left(1+\alpha_q^k\right)\frac{1-\exp\left(-\delta\mu_q^k\right)}{1+\exp\left(-\delta\mu_q^k\right)} + \left(1-\alpha_q^k\right)\frac{1-\exp\left(-\delta\nu_q^k\right)}{1+\exp\left(-\delta\nu_q^k\right)}
\end{bmatrix}}{\lambda\delta(\chi+4)}$$

$$V_q^k = \begin{bmatrix} \sigma^2 I_2 & \sigma^2\alpha_q^k I_2 \\ \sigma^2\alpha_q^k I_2 & \sigma^2 I_2 \end{bmatrix}.$$

Therefore, if $\delta \to 0$ and q is always chosen to be a point in S^0 closest to a fixed $\bar{x} \in V \setminus F$, then

$$\begin{aligned}
m_q^k &\to \hat{u}(\bar{x},k\Delta t)+\hat{f}(\bar{x},k\Delta t) \\
V_q^k &\to \sigma^2\begin{bmatrix} I_2 & \hat{h}(\bar{x})I_2 \\ \hat{h}(\bar{x})I_2 & I_2 \end{bmatrix} = \sigma^2\Sigma^2(\bar{x}).
\end{aligned}$$

Therefore, the following proposition is derived.

Proposition 2: Fix $\delta > 0$ and consider the corresponding Markov chain $\{Q_k, k \ge 0\}$. Denote by $\{Q(t), t \ge 0\}$ the stochastic process that is equal to Q_k on the time interval $[k\Delta t, (k+1)\Delta t)$ for $k \ge 0$. Then, as $\delta \to 0$, $\{Q(t), t \ge 0\}$ converges weakly to the solution $\{\bar{X}(t), t > 0\}$ to (21) defined on $V \setminus F$ with absorption on the boundary $\partial V \cup \partial F$.

As a result, a good approximation to the probability of conflict (22) is given by

$$P_{c,\delta}^V \triangleq P\{Q_k \text{ hits } \partial S_F \text{ before hitting } \partial S_V \text{ within } 0 \le k \le k_f\} \tag{24}$$

where $k_f = \lfloor t_f/\Delta t \rfloor$, for sufficiently small δ. Here, the chain Q_k is assumed to start from a point $\bar{q}$ in S closest to $\hat{X}(0)$.

Remark 6: In a time interval of length $\Delta t = \lambda\delta^2$, the maximal distance that the Markov chain Q_k can travel in any dimension is δ. Thus, given $u_i(x_i,t)$ and V_i for $i = 1, 2$, in order for $\bar{X}(t)$ to be approximated by Q_k, the quantities $[u_i(x_i,t) + f(x_i,t)]_j$, $j = 1, 2$, have to be upper bounded on $V_i \times T$ by $1/\lambda\delta$, which is $2\sigma^2/\delta$ if $\lambda = (2\sigma^2)^{-1}$ is chosen. These conditions put upper bounds on the admissible values of δ.

If the following set of functions is introduced

$$P_{c,\delta}^{(k)}(q) \triangleq P\{Q_{k_f} \in \partial S_F | Q_k = q\}, \quad q \in S$$

$k = 0, \ldots, k_f$, then $P_{c,\delta}^V$ defined in (24) can be computed recursively as follows.

Algorithm 2. Given $X_1(0)$, $X_2(0)$, $u_1(x,t)$, $u_2(x,t)$, and $f(x,t)$, for $x \in \mathbb{R}^2$, $t \in T$:

1) Fix $\delta > 0$ and $\lambda \in (0, 1/(2\sigma^2)]$. Set $\Delta t = \lambda\delta^2$. Define the Markov chain $\{Q_k, k \ge 0\}$ with state space $S = (V \setminus F) \cap \delta\mathbb{Z}^4$ and transition probabilities given by (23).
2) Initialize $P_{c,\delta}^{(k_f)}$ by

$$P_{c,\delta}^{(k_f)}(q) = \begin{cases} 1, & \text{if } q \in \partial S_F \\ 0, & \text{otherwise.} \end{cases}$$

3) For $k = k_f - 1, \ldots, 0$, compute $P_{c,\delta}^{(k)}$ from $P_{c,\delta}^{(k+1)}$ as follows: for each $q \in S$

$$P_{c,\delta}^{(k)}(q) = \begin{cases} P_{c,\delta,\text{new}}^{(k)}(q), & \text{if } q \in S^0 \\ 1, & \text{if } q \in \partial S_F \\ 0, & \text{if } q \in \partial S_V \end{cases}$$

where

$$\begin{aligned}
P_{c,\delta,\text{new}}^{(k)}(q) = & p_{oo}^k(q)P_{c,\delta}^{(k+1)}(q) + p_{ll}^k(q)P_{c,\delta}^{(k+1)}(q_{ll}) \\
& + p_{rr}^k(q)P_{c,\delta}^{(k+1)}(q_{rr}) + p_{lr}^k(q)P_{c,\delta}^{(k+1)}(q_{lr}) \\
& + p_{rl}^k(q)P_{c,\delta}^{(k+1)}(q_{rl}) + p_{dd}^k(q)P_{c,\delta}^{(k+1)}(q_{dd}) \\
& + p_{uu}^k(q)P_{c,\delta}^{(k+1)}(q_{uu}) + p_{du}^k(q)P_{c,\delta}^{(k+1)}(q_{du}) \\
& + p_{ud}^k(q)P_{c,\delta}^{(k+1)}(q_{ud}).
\end{aligned}$$

4) Choose a point $\bar{q}$ in S that is closest to $\hat{X}(0) = (X_1(0), X_2(0))$ and output $P_{c,\delta}^V = P_{c,\delta}^{(0)}(\bar{q})$.

By Proposition 2, $P_{c,\delta}^{V}$ converges to P_c^V as $\delta \to 0$, thus providing a good approximation of the probability of conflict when δ is sufficiently small.

Remark 7: The size of the state space S is of the order of $1/\delta^4$. Since the number of iterations is $k_f \simeq t_f/\Delta t = O(1/\delta^2)$, the running time of Algorithm 2 grows as $O(1/\delta^6)$ as $\delta \to 0$. Due to the increase in the state space dimension, the running time of Algorithm 2 is significantly larger than that of Algorithm 1, a price paid for the generality of Algorithm 2.

One can also extend the approach to the case when the aircraft initial positions are uncertain in a completely similar way as in Section III. The details are omitted here.

Remark 8: There are infinitely many possible ways of defining the transition probabilities for $\{Q_k, k \geq 0\}$ on S such that Proposition 2 still holds. The choice in (23) is "sparse" in the sense that starting from a point in S^0 the chain can only jump to eight of its neighboring grid points. The advantage of such a choice is that each iteration step in Algorithm 2 takes less time. The disadvantage is that if the chain starts from a certain point, it can only reach approximately one half of the grid points in S, i.e., those points in S with the same parity as the starting point. Hence, the level curves of $P_{c,\delta}^{(0)}$ computed by Algorithm 2 tend to be saw-like. One solution can be to smooth $P_{c,\delta}^{(0)}$ by passing it through a low pass filter. This is equivalent to saying that there is some uncertainty in the aircraft initial positions.

B. Examples

If Assumption 1 holds, experiments show that Algorithm 2 returns similar results to those of Algorithm 1. Hence, examples for which Assumption 1 fails are presented here.

Example 4: Consider two aircraft that are trying to follow the same straight path, namely, the $[x]_1$ coordinate axis of the plane, flying along it from left to right at different constant speeds during the time interval $T = [0, 20]$. The velocity profiles of the two aircraft are given by

$$u_1(x,t) = \begin{bmatrix} 4 \\ 0 \end{bmatrix} + \begin{bmatrix} 0 \\ -a[x]_2 \end{bmatrix} \quad u_2(x,t) = \begin{bmatrix} 2 \\ 0 \end{bmatrix} + \begin{bmatrix} 0 \\ -a[x]_2 \end{bmatrix}$$

for $x \in \mathbb{R}^2$, $t \in T$, where the parameter a determines the strength of the feedback control of the pilots or onboard controllers to stabilize the cross-track deviations $[x_i]_2$, $i = 1, 2$, toward 0.

Suppose that the safe distance is $r = 3$. The parameter σ and the function $\hat{h}$ are, respectively, $\sigma = 2$ and $\hat{h}((x_1, x_2)) = \exp(-\|x_2 - x_1\|)$, $x_1, x_2 \in \mathbb{R}^2$. The wind field $f(x,t)$ is assumed to be time invariant but nonlinear in x

$$f(x,t) = \begin{bmatrix} \frac{\exp\left(\frac{[x]_1+20}{2}\right)-1}{\exp\left(\frac{[x]_1+20}{2}\right)+1} \\ 0 \end{bmatrix}.$$

Under this wind field model, the wind direction is along the $[x]_1$ axis from right to left on the half-plane with $[x]_1 < -20$, and from left to right on the half-plane with $[x]_1 > -20$. The maximal strength $\| f(x,t)\|$ of the wind is 1, which is achieved when $[x]_1 \to \pm\infty$.

Based on the above parameters, the domains V_1 and V_2 are chosen to be the open rectangles $V_1 = (-100, 30) \times (-24, 24)$ and $V_2 = (-60, 80) \times (-16, 16)$. Finally, set $\lambda = (2\sigma^2)^{-1} = 0.125$ and $\delta = 1.5$ so that $\Delta t = \lambda\delta^2 = 9/32$.

In Figs. 4 and 5, the level curves of the probability of conflict (24) are plotted as a function of the initial position of aircraft 1, for five different initial positions of aircraft 2: $(-40, 0)$; $(-30, 0)$; $(-20, 0)$; $(0, 0)$; and $(20, 0)$, from top to bottom. Fig. 4 corresponds to the case when $a = 0$ (no feedback control in both aircraft velocity profiles), and Fig. 5 to the case when $a = 0.05$ (with stabilizing feedback control). In each figure, the probability of conflict as computed by Algorithm 2 for a fixed initial position of aircraft 2 is visualized in two figures on the same row: The original version is shown in the left one and, to overcome the roughness in the level curves caused by the coarse grid size $\delta = 1.5$, shown in the right one is a smoothed version whose value at each $z \in V_1 \cap \delta\mathbb{Z}^2$ is the average of the original probability of conflict at z and at its four immediate neighbors z_l, z_r, z_d, z_u. In effect, this is equivalent to passing the original probability of conflict through a low pass filter $1/5 \begin{bmatrix} 0 & 1 & 0 \\ 1 & 1 & 1 \\ 0 & 1 & 0 \end{bmatrix}$, or assuming that there is uncertainty in the initial position of aircraft 1, such that it is equally probable that aircraft 1 occupies its current position and the four immediate neighboring grid points.

In Fig. 4 (or Fig. 5), it can be seen that, unlike in the simplified case in Section III, the probability of conflict, in general, depends on the initial positions of both aircraft, not just on their initial relative position, for otherwise the level curves in the plots of Fig. 4 (or Fig. 5) would be all identically shaped and one could be obtained from another by a proper translation, which is obviously not the case in either figure. In addition, it is noted that this dependence of the probability of conflict on the initial positions of both aircraft rather than simply their relative position is more eminent at those places where there is a large acceleration (or deceleration) in wind components, i.e., at those places with strong nonlinearity in the wind field. Observe that in this example, the relative velocity of the two aircraft can be expressed as a function of the aircraft relative position, hence, it is the nonlinearity of the wind field that makes Algorithm 1 not applicable (see Remark 3). If the nonlinearity of the wind field is relatively small, Algorithm 1 can be used instead of Algorithm 2, significantly reducing the computation time. Finally, by comparing Fig. 4 with Fig. 5, it can be seen that in Fig. 5, the regions with high probability of conflict are more extended than their counterparts in Fig. 4. This is as expected since the presence of the feedback control will render some previously safe configurations unsafe as both aircraft tend to converge to the same nominal path.

V. Probability of Intrusion Into a Protected Area

The approach proposed to estimate the probability of conflict for a two-aircraft encounter can be generalized to estimate the probability of intrusion of an aircraft into a protected area of the airspace with an arbitrary shape.

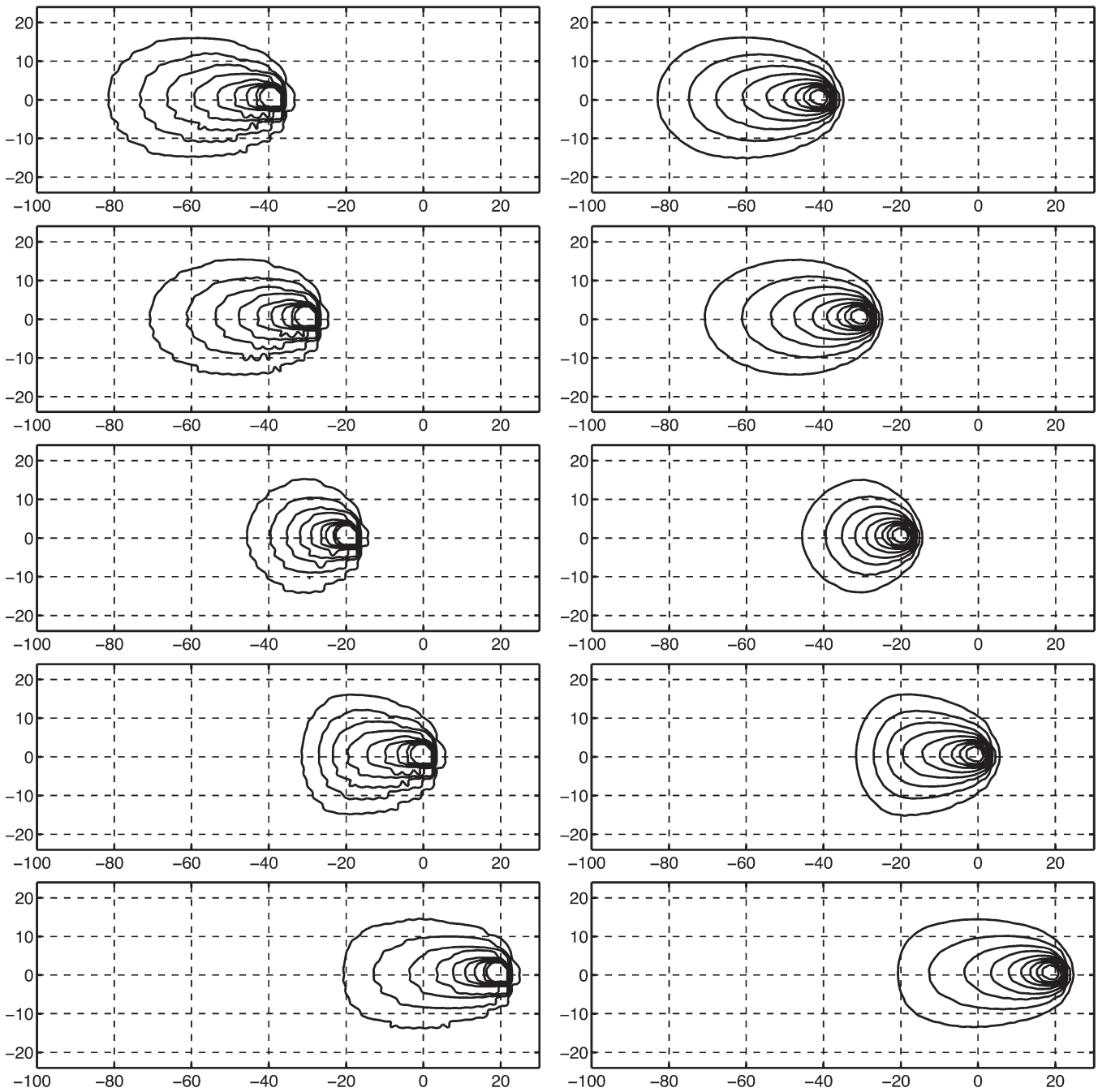

Fig. 4. Level curves of the estimated probability of conflict over the time horizon [0, 20] as a function of the initial position of aircraft 1 for fixed initial position of aircraft 2 [from top to bottom: $X_2(0) = (-40, 0)$, $(-30, 0)$, $(-20, 0)$, $(0, 0)$, and $(20, 0)$]. In each case, the right figure shows the level curves of a smoothed version of the original probability of conflict shown in the left figure. No feedback $(a = 0)$.

Consider the stochastic differential equation (4) describing the position $X \in \mathbb{R}^2$ of a single aircraft with a certain velocity profile within some look-ahead time horizon T. By following a similar reasoning as in Sections III and IV, one can show that the process X has the same distribution as a process $\tilde{X}$ solving the stochastic differential equation

$$\mathrm{d}\tilde{X}(t) = u(\tilde{X}, t)\mathrm{d}t + f(\tilde{X}, t)\mathrm{d}t + \sigma \mathrm{d}\tilde{W}(t) \qquad (25)$$

with initial condition $\tilde{X}(0) = X(0)$, where $\tilde{W}$ is a standard 2-D Brownian motion. Denote by D an arbitrarily shaped closed region of $\mathbb{R}^2$ that the aircraft should avoid, and by U an open subset of $\mathbb{R}^2$ containing D and large enough such that whenever the aircraft wanders outside U, the situation can be declared to be safe. Then, the probability of intrusion of the aircraft into the protected area D over the time horizon T can be defined as the probability that $\tilde{X}$ hits D before it (ever) hits U^c within the time interval T. By adopting the same procedure as in Section III, a Markov chain $\{Q_k, k \geq 0\}$ can be constructed on the grid space $(U \setminus D) \cap \delta\mathbb{Z}^2$ so that as the discretization size $\delta \to 0$, Q_k converges weakly to $\tilde{X}(t)$. Then, the probability of intrusion for $X(t)$ can be approximated by the corresponding probability for $\{Q_k, k \geq 0\}$ for small enough δ. Since this procedure is

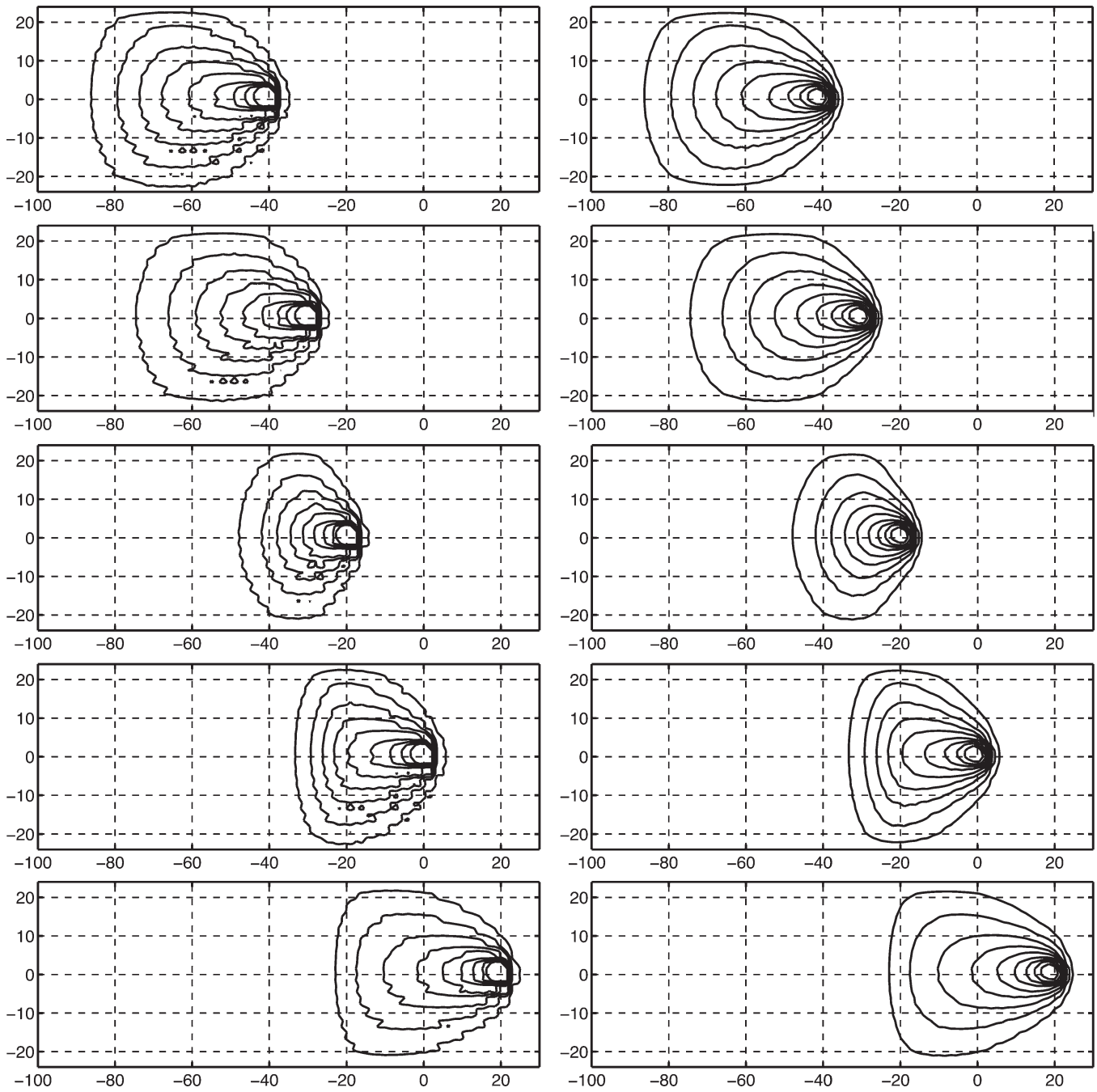

Fig. 5. Level curves of the estimated probability of conflict over the time horizon [0, 20] as a function of the initial position of aircraft 1 for fixed initial position of aircraft 2 [from top to bottom: $X_2(0) = (-40, 0)$, $(-30, 0)$, $(-20, 0)$, $(0, 0)$, and $(20, 0)$]. In each case, the right figure shows the level curves of a smoothed version of the original probability of conflict shown in the left figure. With feedback $(a = 0.05)$.

entirely similar to the one introduced before without any added complexity, the details are omitted.

VI. Conclusion and Future Direction

Correlation of the wind perturbations to the aircraft motions has been largely ignored in the current literature on aircraft conflict detection. In this paper, a model of a two-aircraft encounter with a random field term is introduced to address this issue. Based on this model, one can effectively estimate the probability of conflict by using a Markov chain approximation scheme. Simulation results show that the correlation of wind perturbations does affect the values of the probability of conflict.

One advantage of the approach proposed in this paper is that, upon completion, one has the probability of conflict not only at the current time, but also at all future time instants, which eliminates the need for recomputation if the flight plans remain unchanged. The approach can also be extended to address more general cases such as, for example, computing the probability of conflict when the current aircraft positions are uncertain, or estimating the probability of intrusion into a protected area of the airspace with an arbitrary shape.

One possible future direction is to extend the introduced algorithms to the case of more realistic aircraft dynamics, such as second-order feedback control, and to test them with actual flight and atmospheric data. It would also be interesting to study how the computed probability of conflict can be used to assist in the decision process for conflict resolution.

APPENDIX
EXISTENCE OF THE RANDOM FIELD MODELING THE STOCHASTIC WIND COMPONENT

In this section, we study the existence of a random field $B(\cdot,\cdot)$ on $\mathbb{R}^2 \times T$ with the following properties:

1) For each fixed $x \in \mathbb{R}^2$, $B(x,\cdot)$ is a standard 2-D Brownian motion.
2) $B(\cdot,\cdot)$ is time increment independent.
3) $\{B(x,t_2)-B(x,t_1)\}_{x\in\mathbb{R}^2}$, for any $t_1, t_2 \in T$ with $t_1 \le t_2$, is an (uncountable) collection of Gaussian random variables with zero mean and covariance

$$E\left\{[B(x_1,t_2)-B(x_1,t_1)]\,[B(x_2,t_2)-B(x_2,t_1)]^{\mathrm{T}}\right\} = h(x_1-x_2)(t_2-t_1)I_2 \quad \forall x_1, x_2 \in \mathbb{R}^2$$

for some nonnegative definite $h:\ \mathbb{R}^2 \to \mathbb{R}$ with $h(x) = h(-x)\ \forall x \in \mathbb{R}^2$, and $h(0) = 1$.

However, instead of constructing $B(\cdot,\cdot)$ on $\mathbb{R}^2 \times T$ directly, for each $\delta > 0$, a random field $B_\delta(\cdot,\cdot)$ on $\delta\mathbb{Z}^2 \times T$ shall be constructed, satisfying the above properties on $\delta\mathbb{Z}^2 \times T$, where $\delta\mathbb{Z}^2$ denotes the integer grid in $\mathbb{R}^2$ scaled by δ. In particular, if the following correlation functions are defined

$$R(x_1,x_2;t_1,t_2) \triangleq E\left\{[B(x_1,t_2)-B(x_1,t_1)]\,[B(x_2,t_2)-B(x_2,t_1)]^{\mathrm{T}}\right\} \quad \forall x_1, x_2 \in \mathbb{R}^2$$

$$R_\delta(z_1,z_2;t_1,t_2) \triangleq E\left\{[B_\delta(z_1,t_2)-B_\delta(z_1,t_1)]\,[B_\delta(z_2,t_2)-B_\delta(z_2,t_1)]^{\mathrm{T}}\right\} \quad \forall z_1, z_2 \in \delta\mathbb{Z}^2$$

for $t_1, t_2 \in T$ with $t_1 \le t_2$, then the constructed $B_\delta(\cdot,\cdot)$ is such that $R_\delta(x_1,x_2;t_1,t_2)$ coincides with $R(x_1,x_2;t_1,t_2)$ for $x_1, x_2 \in \delta\mathbb{Z}^2$. Thus, $B_\delta(\cdot,\cdot)$ can replace $B(\cdot,\cdot)$ for the purpose of this paper, where the state space $\mathbb{R}^2$ is discretized into $\delta\mathbb{Z}^2$ for the Markov chain approximation.

Fix a $\delta > 0$. Let $W_\delta(z,\cdot)$, $z \in \delta\mathbb{Z}^2$, be a collection of independent 2-D standard Brownian motions. Let $\rho:\ \delta\mathbb{Z}^2 \to \mathbb{R}$ be a function to be determined later. For each $t \in T$, define $B_\delta(\cdot,t) \triangleq W_\delta(\cdot,t) * \delta\rho(\cdot)$ where $*$ denotes convolution over $\delta\mathbb{Z}^2$, i.e.,

$$B_\delta(z,t) \triangleq \sum_{z'\in\delta\mathbb{Z}^2} \delta\rho(z-z')W_\delta(z',t) \quad \forall z \in \delta\mathbb{Z}^2.$$

Then, the correlation function of $B_\delta(\cdot,t)$ can be calculated as

$$\begin{aligned} &R_\delta(z_1,z_2;t_1,t_2) \\ &\quad = E\left\{[B_\delta(z_1,t_2)-B_\delta(z_1,t_1)]\,[B_\delta(z_2,t_2)-B_\delta(z_2,t_1)]^{\mathrm{T}}\right\} \\ &\quad = E\Bigg\{\sum_{z_1',z_2'\in\delta\mathbb{Z}^2} \delta^2\rho(z_1-z_1')\rho(z_2-z_2') \\ &\qquad \cdot[W_\delta(z_1',t_2)-W_\delta(z_1',t_1)][W_\delta(z_2',t_2)-W_\delta(z_2',t_1)]^{\mathrm{T}}\Bigg\} \\ &\quad = \sum_{z_1'\in\delta\mathbb{Z}^2} \delta^2\rho(z_1-z_1')\rho(z_2-z_1')(t_2-t_1)I_2 \\ &\quad = \sum_{z'\in\delta\mathbb{Z}^2} \delta^2\rho(z_1-z_2+z')\rho(z')(t_2-t_1)I_2 \end{aligned}$$

for all $z_1, z_2 \in \delta\mathbb{Z}^2$, where in the second equality, the spatial independence of $W_\delta(\cdot,t)$ over $\delta\mathbb{Z}^2$ is used. In order that $R_\delta(z_1,z_2;t_1,t_2) = R(z_1,z_2;t_1,t_2)\ \forall z_1, z_2 \in \delta\mathbb{Z}^2$, ρ needs to be chosen such that

$$\sum_{z'\in\delta\mathbb{Z}^2} \delta^2\rho(z+z')\rho(z') = h(z) \quad \forall z \in \delta\mathbb{Z}^2. \tag{26}$$

Denote by $\mathcal{F}[\rho]$ the Fourier transform of ρ defined as $\mathcal{F}[\rho](\omega_1,\omega_2) \triangleq \sum_{j,k\in\mathbb{Z}} \rho(\delta j,\delta k)\mathrm{e}^{-i(j\omega_1+k\omega_2)} \quad \forall \omega_1,\omega_2 \in [-\pi,\pi]$. Similarly, $\mathcal{F}[h|_{\delta\mathbb{Z}^2}]$ denotes the Fourier transform of h restricted on $\delta\mathbb{Z}^2$. Then, assuming the existence of both $\mathcal{F}[\rho]$ and $\mathcal{F}[h|_{\delta\mathbb{Z}^2}]$, (26) is equivalent to $\delta^2|\mathcal{F}[\rho]|^2 = \mathcal{F}[h|_{\delta\mathbb{Z}^2}]$. Since h is nonnegative definite on $\mathbb{R}^2$, hence, on $\delta\mathbb{Z}^2$, by the Bochner Theorem, for all $j, k \in \mathbb{Z}$

$$h(\delta j,\delta k) = \int_{-\pi}^{\pi}\int_{-\pi}^{\pi} \mathrm{e}^{i(j\omega_1+k\omega_2)}\sigma(\omega_1,\omega_2)\mathrm{d}\omega_1\mathrm{d}\omega_2$$

for some finite measure with (generalized) density function $\sigma \ge 0$. Thus, $\mathcal{F}[h|_{\delta\mathbb{Z}^2}](\omega_1,\omega_2) = 4\pi^2\sigma(-\omega_1,-\omega_2)$ is real and positive for $\omega_1,\omega_2 \in [-\pi,\pi]$. As a result, $\sqrt{\mathcal{F}[h|_{\delta\mathbb{Z}^2}]}$ exists, and the desired ρ satisfying (26) can be obtained via inverse Fourier transformation as

$$\rho = \delta^{-1}\mathcal{F}^{-1}\left\{\sqrt{\mathcal{F}[h|_{\delta\mathbb{Z}^2}]}\right\}. \tag{27}$$

Note that ρ as obtained in (27) must be real since $\sqrt{\mathcal{F}[h|_{\delta\mathbb{Z}^2}]}$ is a real even function.

To sum up, for each $\delta > 0$, a random field $B_\delta(\cdot,\cdot)$ on $\delta\mathbb{Z}^2 \times T$, whose correlation function coincides with that of the desired $B(\cdot,\cdot)$ over $\delta\mathbb{Z}^2 \times T$, can be constructed, provided that h satisfies the condition

$$\mathcal{F}^{-1}\left\{\sqrt{\mathcal{F}[h|_{\delta\mathbb{Z}^2}]}\right\} \text{ exists for all } \delta > 0. \tag{28}$$

The choice of h in this paper, $h(x) = \exp(-\beta\|x\|)$, $\beta > 0$, can be verified to satisfy this condition. As for properties 1) and 2), they directly follow from the definition of $B_\delta(\cdot,t)$ as a sum

of independent Brownian motions and from property 3) with $h(0) = 1$.

Remark 9: A random field $\hat{B}_\delta(\cdot,\cdot)$ on $\mathbb{R}^2 \times T$ can be constructed from $B_\delta(\cdot,\cdot)$

$$\hat{B}_\delta\left(\begin{bmatrix}x\\y\end{bmatrix},t\right) \triangleq B_\delta\left(\begin{bmatrix}\delta\lfloor\frac{x}{\delta}\rfloor\\ \delta\lfloor\frac{y}{\delta}\rfloor\end{bmatrix},t\right) \quad \forall x,y\in\mathbb{R}, t\in T.$$

The correlation function of $\hat{B}_\delta(\cdot,\cdot)$ is stair-like and coincides with that of $B(\cdot,\cdot)$ on $\delta\mathbb{Z}^2 \times T$.

ACKNOWLEDGMENT

The authors would like to thank the anonymous reviewers for their useful comments and suggestions.

REFERENCES

[1] Radio Technical Commission for Aeronautics, "Minimum operational performance standards for traffic alert and collision avoidance system (TCAS) airborne equipment," RTCA, Washington, DC, Tech. Rep. RTCA/DO-185, Sep. 1990, consolidated edition.

[2] J. Kuchar and L. Yang, "A review of conflict detection and resolution modeling methods," *IEEE Trans. Intell. Transp. Syst., Special Issue on Air Traffic Control, Part I*, vol. 1, no. 4, pp. 179–189, Dec. 2000.

[3] L. Yang and J. Kuchar, "Using intent information in probabilistic conflict analysis," in *Proc. American Institute Aeronautics and Astronauts (AIAA) Guidance, Navigation and Control Conf.*, Boston, MA, Aug. 1998, p. 797.

[4] R. Paielli and H. Erzberger, "Conflict probability estimation for free flight," *J. Guid. Control Dyn.*, vol. 20, no. 3, pp. 588–596, 1997.

[5] M. Prandini, J. Hu, J. Lygeros, and S. Sastry, "A probabilistic approach to aircraft conflict detection," *IEEE Trans. Intell. Transp. Syst., Special Issue on Air Traffic Control, Part I*, vol. 1, no. 4, pp. 199–220, Dec. 2000.

[6] H. Erzberger, R. Paielli, D. Isaacson, and M. Eshow, "Conflict detection and resolution in the presence of prediction error," in *Proc. 1st USA/Europe Air Traffic Management R&D Seminar*, Saclay, France, 1997.

[7] J. Hu, M. Prandini, and S. Sastry, "Optimal coordinated motions for multiple agents moving on a plane," *SIAM J. Control Optim.*, vol. 42, no. 2, pp. 637–668, 2003.

[8] ——, "Optimal coordinated maneuvers for three dimensional aircraft conflict resolution," *J. Guid. Control Dyn.*, vol. 25, no. 5, pp. 888–900, 2002.

[9] C. Tomlin, G. Pappas, and S. Sastry, "Conflict resolution for air traffic management: A study in multi-agent hybrid systems," *IEEE Trans. Autom. Control*, vol. 43, no. 4, pp. 509–521, Apr. 1998.

[10] F. Medioni, N. Durand, and J. Alliot, "Air traffic conflict resolution by genetic algorithms," in *Proc. Artificial Evolution, European Conf. (AE)*, Brest, France, 1995, pp. 370–383.

[11] J. Krozel and M. Peters, "Strategic conflict detection and resolution for free flight," in *Proc. 36th IEEE Int. Conf. Decision and Control*, San Diego, CA, Dec. 1997, vol. 2, pp. 1822–1828.

[12] P. Menon, G. Sweriduk, and B. Sridhar, "Optimal strategies for free-flight air traffic conflict resolution," *J. Guid. Control Dyn.*, vol. 22, no. 2, pp. 202–211, 1999.

[13] Y. Zhao and R. Schultz, "Deterministic resolution of two aircraft conflict in free flight," in *Proc. American Institute Aeronautics and Astronauts (AIAA) Guidance, Navigation, and Control Conf., AIAA-97-3547*, New Orleans, LA, Aug. 1997, pp. 469–478.

[14] J. Kosecka, C. Tomlin, G. Pappas, and S. Sastry, "Generation of conflict resolution maneuvers for air traffic management," in *Proc. IEEE Conf. Intelligent Robots and Systems*, Grenoble, France, 1997, vol. 3, pp. 1598–1603.

[15] L. Yang and J. Kuchar, "Prototype conflict alerting system for free flight," *J. Guid. Control Dyn.*, vol. 20, no. 4, pp. 768–773, 1997.

[16] J. Hu, J. Lygeros, M. Prandini, and S. Sastry, "Aircraft conflict prediction and resolution using Brownian Motion," in *Proc. 38th IEEE Int. Conf. Decision and Control*, Phoenix, AZ, Dec. 1999, vol. 3, pp. 2438–2443.

[17] J. Kaimal, J. Wyngaard, Y. Izumi, and O. Cote, "Spectral characteristics of surface-layer turbulence," *Q. J. R. Meteorol. Soc.*, vol. 98, no. 417, pp. 563–589, 1972.

[18] R. Milli, P. Niiler, J. Morzel, A. Sybrandy, D. Nychka, and W. Large, "Mesoscale correlation length scales from NSCAT and Minimet," *J. Atmos. Ocean. Technol.*, vol. 20, no. 4, pp. 5137–533, 2003.

[19] R. Cole, C. Richard, S. Kim, and D. Bailey, "An assessment of the 60 km rapid update cycle (RUC) with near real-time aircraft reports," Massachusetts Inst. Technol. (MIT) Lincoln Laboratory, Lexington, MA, Tech. Rep. NASA/A-1, Jul. 1998.

[20] J. Lygeros and M. Prandini, "Aircraft and weather models for probabilistic collision avoidance," in *Proc. 41st IEEE Int. Conf. Decision and Control*, Las Vegas, NV, Dec. 2002, vol. 3, pp. 2427–2432.

[21] J. Hu, M. Prandini, and S. Sastry, "Probabilistic safety analysis in three dimensional aircraft flight," in *Proc. 42nd IEEE Int. Conf. Decision and Control*, Maui, HI, Dec. 2003, vol. 5, pp. 5335–5340.

[22] E. Isaaks and R. Srivastava, *An Introduction to Applied Geostatistics*. New York: Oxford Univ. Press, 1989.

[23] S. Benjamin, K. Brundage, P. Miller, T. Smith, G. Grell, D. Kim, J. Brown, T. Schlatter, and L. Morone, "The Rapid Update Cycle at NMC," in *Proc. 10th Conf. Numerical Weather Prediction*, Portland, OR, Jul. 1994, pp. 566–568.

[24] G. Christakos, *Random Field Models in Earth Sciences*. San Diego, CA: Academic, 1992.

[25] R. Durrett, *Stochastic Calculus*. Boca Raton, FL: CRC Press, 1996.

[26] D. Stroock and S. Varadhan, *Multidimensional Diffusion Process*. New York: Springer-Verlag, 1979.

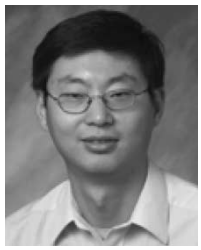

Jianghai Hu (S'99–M'04) received the B.E. degree in automatic control from Xi'an Jiaotong University, Xi'an, PR China, in 1994, and the M.A. degree in mathematics and the Ph.D. degree in electrical engineering from the University of California, Berkeley, in 2002 and 2003, respectively.

He is currently an Assistant Professor at the School of Electrical and Computer Engineering, Purdue University, West Lafayette, IN. His research interests include hybrid systems, multiagent coordinated control, control of systems with uncertainty, and applied mathematics and probability theory.

Maria Prandini (S'96–M'00) received the Laurea degree in electrical engineering from the Politecnico of Milano, Milan, Italy, in 1994, and the Ph.D. degree in electrical engineering from the University of Brescia, Brescia, Italy, in 1998.

From March to July 1998, she was a visiting scholar at the Delft University of Technology, Delft, the Netherlands. From August 1998 to July 1999, she was a visiting postdoctoral researcher at the Electrical Engineering and Computer Sciences Department, University of California at Berkeley. She is currently an Assistant Professor at the Politecnico of Milano, Milan, Italy. Her research interests include identification and adaptive control of stochastic systems, statistical learning theory for system analysis and design, coordination and control of multiagent systems, air traffic management, and verification of hybrid systems.

Shankar Sastry (S'79–M'80–SM'90–F'95) received the M.S. degree in electrical engineering (honoris causa) from Harvard University, Cambridge, MA, in 1994, and the Ph.D. degree in electrical engineering from the University of California, Berkeley, in 1981.

From 1980 to 1982, he was an Assistant Professor at the Massachusetts Institute of Technology, Cambridge, MA. In 2000, he was Director of the Information Technology Office at the Defense Advanced Research Projects Agency, Arlington, VA. From 2001 to 2004, he was the Chairman of the Department of Electrical Engineering and Computer Sciences, University of California. He is currently the NEC Distinguished Professor of Electrical Engineering and Computer Sciences and Bioengineering, University of California. He has held visiting appointments at the Australian National University, Canberra, the University of Rome, Scuola Normale and University of Pisa, the CNRS laboratory LAAS in Toulouse (poste rouge), Professor Invite at Institut National Polytechnique de Grenoble (CNRS laboratory VERIMAG), and as a Vinton Hayes Visiting fellow at the Center for Intelligent Control Systems at MIT. His research interests include embedded and autonomous software, computer vision, computation in novel substrates such as DNA, nonlinear and adaptive control, robotic telesurgery, control of hybrid systems, embedded systems, sensor networks, and biological motor control.

Prof. Sastry received the President of India Gold Medal in 1977, the IBM Faculty Development Award for 1983–1985, the NSF Presidential Young Investigator Award in 1985, the Eckman Award of the of the American Automatic Control Council in 1990, the distinguished Alumnus Award of the Indian Institute of Technology in 1999, and the David Marr prize for the best paper at the International Conference in Computer Vision in 1999. In 2001, he was elected into the National Academy of Engineering for pioneering contributions to the design of hybrid and embedded systems. He has served as Associate Editor for IEEE TRANSACTIONS ON AUTOMATIC CONTROL, IEEE Control System Magazine, IEEE TRANSACTIONS ON CIRCUITS AND SYSTEMS, Systems and Control Letters, and the Journal of Mathematical Systems, Estimation and Control, and he is an Associate Editor of the IMA Journal of Mathematical Control and Information and the International Journal of Adaptive and Optimal Control.